Ocean Engineering 108 (2015) 155–163

Contents lists available at ScienceDirect

Ocean Engineering

journal homepage: www.elsevier.com/locate/oceaneng

The impact of diffuser augmentation on a tidal stream turbine

N.W. Cresswell [a,*], G.L. Ingram [a,1], R.G. Dominy [b,1]

[a] School of Engineering and Computing Sciences, Durham University, Durham DH1 3DE, UK
[b] Department of Mechanical & Construction Engineering, Northumbria University, Newcastle upon Tyne NE1 8ST, UK

ARTICLE INFO

Article history:
Received 16 February 2015
Received in revised form
30 June 2015
Accepted 21 July 2015
Available online 24 August 2015

Keywords:
Tidal stream turbine
Diffuser augmentation
Wake recovery
Yaw

ABSTRACT

The results from an experimental study of a model diffuser augmented tidal stream turbine are presented with a particular focus on the impact of the diffuser upon the turbine's performance in yawed flows. This study is the first to examine yaw effects with quantification of blockage corrections and is the first study of the wake recovery characteristics of such devices. The device was designed using an innovative optimisation procedure resulting in a diffuser that was able to maintain the turbine's performance to yaw angles of up to $\pm 30^{\circ}$. It is shown that the diffuser's performance is strongly influenced by its length to diameter ratio and by the jet flow that develops through the turbine's tip gap. Although the performance characteristics of an individual turbine can be significantly improved by diffuser augmentation under yawed flow, a wake recovery rate that is less than half that of a bare rotor raises doubts about their suitability for array deployment.

1. Introduction

It is estimated that the UK could produce 15–20% of its electricity demand from tidal resources (Callaghan, 2006). With such a large resource available there has been increased research in tidal stream generation. The conversion technology is at an early stage of development and questions remain regarding the design, cost and productive capacity of such devices.

Much of the existing conversion technology used for tidal stream generators has its origin in the wind energy industry (Fraenkel, 2002; Batten et al, 2007; Bahaj et al., 2007). Many possible device configurations have been proposed with horizontal axis turbines receiving most research attention (Khan et al., 2009).

Diffuser augmentation of wind turbines has been mooted since the late 1970s (Flay et al., 1998) and there is experimental data which demonstrates potential performance enhancements (Igra, 1977, 1981; Flay et al., 1998, Phillips, 2003; Abe et al., 2005; Ohya et al., 2008; Ohya and Karasudani, 2010). This concept has been largely rejected as impractical due to structural loadings, associated costs, doubts over generation performance and visual intrusion (Lawn, 2003; van Bussel, 2007; Gaden and Bibeau, 2010). For smaller, less visually intrusive tidal turbines, in a predictable flow regime, the case for diffuser augmentation is stronger. Questions over the fluid dynamics and performance of diffuser augmented devices remain however.

The study of diffuser augmented tidal stream devices has been approached by a number of authors who looked to maximise the power output (Munch et al., 2009; Gaden and Bibeau, 2010; Shives and Crawford, 2010; Belloni and Willden, 2011; Fleming et al., 2011; Luquet et al., 2011; Reinecke et al., 2011). Secondary characteristics which affect the power generation capabilities of diffuser augmented tidal stream devices, such as performance in yawed flows and wake recovery have not been investigated however.

Research into the yaw performance of diffuser augmented wind turbines has been presented by a number of authors (Kogan and Seginer, 1963; Foreman and Gilbert, 1979; Igra, 1981; Phillips, 2003). There is agreement that diffusers maintain device performance at yaw, but the producing mechanism and extent are disputed. Igra (1981) stated that the performance is due to an increase in "lift" from the diffuser's annular wing section, whilst Phillips (2003) stated that it was due to the slotted design of the diffuser, with the slot flow increasing boundary layer momentum. The range of angles over which the performance is maintained extends from $\pm 15^{\circ}$ (Phillips, 2003) to $\pm 30^{\circ}$ (Kogan and Seginer, 1963), with no agreement reached on the performance mechanism. There are also questions raised by the authors about the validity of the findings, since in many cases the devices caused a significant blockage within their respective test sections, with no corrections applied (Igra, 1981; Phillips, 2003).

Wind turbine wake structure has been studied extensively, with summaries presented by Crespo et al. (1999), Vermeer et al. (2003) and Sorensen (2011). The wake structure of horizontal axis tidal stream turbines has also been the subject of study (Bahaj

* Corresponding author. Tel.: +44 191 33 42459.
E-mail addresses: n.w.cresswell@durham.ac.uk (N.W. Cresswell), g.l.ingram@durham.ac.uk (G.L. Ingram), robert.dominy@northumbria.ac.uk (R.G. Dominy).
[1] Tel.: +44 191 33 42428.

http://dx.doi.org/10.1016/j.oceaneng.2015.07.033

et al., 2007; Harrison et al., 2009; Maganga et al., 2010; Myers and Bahaj, 2010; Turnock et al., 2011; Mycek et al., 2014). The wake of a diffuser augmented turbine has received little attention, with the experimental and numerical work of Abe et al. (2005) and Ohya et al. (2012) respectively, on the flow within the cavity of a flanged diffuser structure and that of Grumman Aerospace (Oman et al., 1977) on the exit plane flow of a multi-slotted diffuser being the only studies to the author's knowledge. These studies concentrated on the flow within the cavity and immediately post-exit, but the study of the far wake of a diffuser augmented turbine has not previously been attempted.

This paper investigates the effects of flow yaw on the performance of diffuser augmented turbines and examines the factors which drive this. It also examines the effect of diffuser augmentation on wake propagation and recovery. The implications of these properties of diffuser augmented devices on power generation are also discussed.

2. Experimental methodology

2.1. Test facilities

Testing was undertaken in the 2 m^2 wind tunnel of the School of Engineering at Durham University. The tunnel is a 3/4 open-jet, open-return wind tunnel with an inlet contraction ratio of 7.7:1. The wind tunnel is fitted with an under floor turntable and a three axis overhead gantry traverse system, which is used to control the position of a five hole pressure probe. The maximum blockage in the tunnel, when the diffuser and rotor were operated together, results in a jet area blockage of 9.8%. For the tunnel type and dimensions used the blockage corrections to the velocity field are of the order of 1.18% (Garner et al., 1966; Ewald, 1998).

2.2. Apparatus

The turbine was attached to an AXI5330/24 three phase permanent magnet motor, which was connected to a traverse controlled, coil based variable resistance bank to enable speed control and power takeoff. The motor was attached to an Omega TQM301 reaction torque transducer. The rotational speed was captured using an Optek OPB704 reflective phototransistor, triggered by markings on the drivetrain.

Pressure measurements were taken using Sensortechnics HCLA12X5DB transducers attached to the surface static pressure tappings via pressure tubing. The five hole probe was operated as detailed by Oettle (2013). All data were logged using a National Instruments USB6218 datalogger at a frequency of 2048 Hz.

2.3. Rotor geometry

The rotor geometry was designed to be representative of current designs whilst remaining as simple as possible for ease of modelling and construction. The rotor had three blades, with a tip radius of 174 mm. The blades were constructed from ABS plastic using a Makerbot Replicator, and polished for a smooth surface finish. The blades were developed from a NACA63818 blade section, with a rounded trailing edge to facilitate manufacture. The geometry of the blade section can be seen, along with the NACA63818 section in Fig. 1, with the section's lift and drag performance obtained through CFD analyses in Fig. 2. The CFD simulations were performed in 2D on a structured mesh using ANSYS Fluent with the Transition SST turbulence model and full details of these are given by Cresswell (2015). The details of the blade design, with the linear distributions of blade chord (c) and pitch can be seen in Table 1.

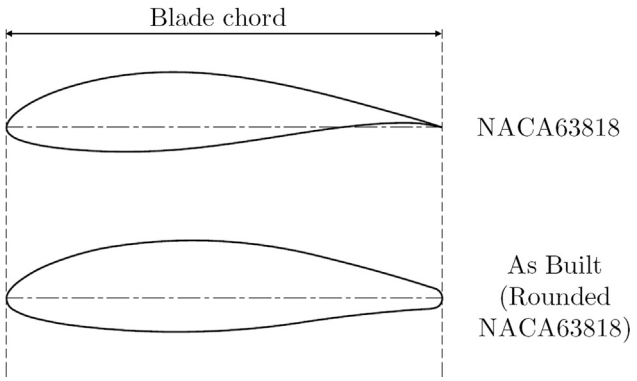

Fig. 1. NACA63818 and as built blade cross sections.

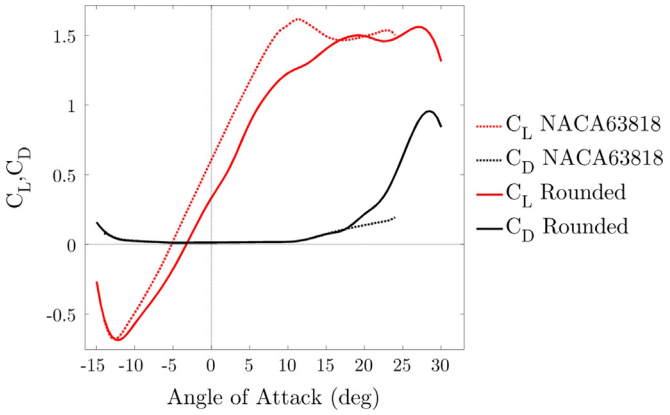

Fig. 2. NACA63818 and rounded NACA63818 lift and drag coefficients against the angle of attack at a Reynolds number of 2.45×10^5 (Cresswell, 2015).

Table 1
Blade geometry details for the experimental blade sets.

r/R_{Ro}	c/R_{Ro}	Pitch (deg)
0.20	0.143	29.49
0.30	0.137	26.12
0.40	0.131	22.74
0.50	0.126	19.37
0.60	0.120	16.00
0.70	0.115	12.62
0.80	0.109	9.25
0.90	0.103	5.87
1.00	0.098	2.50

2.4. Diffuser geometry

The diffuser geometry was created using an optimisation based around CFD, a Kriging surrogate model and a genetic algorithm. Use of a surrogate model and genetic algorithm allows for reduced computational time compared to a genetic algorithm alone (Jeong et al., 2005; Li, 2008).

The device is a uni-directional diffuser augmented horizontal axis tidal turbine, which was assumed to be mounted at mid-depth of a tidal channel. The depth of the channel was taken to be 30 m, which is the mean channel depth in which it is possible to drive monopile foundations (Fraenkel, 2007). Fig. 3 shows the assumed tidal channel and referenced dimensions. The diameter of the device was determined by the need for rotation to face the reversed tidal current, under the constraint that there should be a clearance of 2 m between the device, the seabed and the free surface during rotation and 5 m during operation.

The optimisation was undertaken using seawater properties provided by Sharqawy et al. (2010), at a temperature of 5 °C and a salinity of 35 g/kg, resulting in a density of 1028 kg/m^3 and a dynamic viscosity of 1.6345×10^{-3} Pas. The optimisation was conducted at a freestream velocity of 2.75 m/s as this is a representative value for the rated velocity of existing tidal devices (Bedard, 2005).

The geometry was defined using a number of points, with the coordinates defined by a Latin hypercube experimental design, as control points for a Non-Uniform Rational Basis Splines (NURBS). A uniform actuator disc turbine model was specified in the diffuser throat, with a 5% tip gap and a pressure drop of 45% of the dynamic head. The geometries were examined using CFD, with the power outputs used to construct a Kriging surrogate model using the Design and Analysis of Computational Experiments (DACE) Matlab toolbox (Lophaven et al., 2002). The CFD was performed using 2D axisymmetric simulations in Ansys Fluent with the Transition SST turbulence model. The meshes were created automatically using fully unstructured meshing with refinement in the wake and along surfaces such that the y^+ value was always below 5. Full details of the CFD meshing and solution parameters are provided by Cresswell (2015).

The Kriging model generated from the CFD results was searched using a genetic algorithm, the best design extracted and examined using CFD, with the results used to update the Kriging model. This procedure was iterated until the Kriging predictor and the CFD results were within 1% of one another, at which point the optimum was said to have been found.

Fig. 4 shows the final experimental geometry in cross section, and locations of the surface static pressure tappings and rotor. A view of the combined diffuser and rotor device within the wind tunnel, along with the definition of the yaw angles and turbine rotation can be seen in Fig. 5. The outer radius of the diffuser, which occurs at its trailing edge, was 250 mm for this 1/40 scale model.

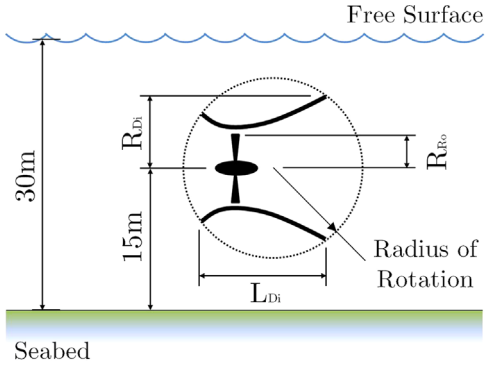

Fig. 3. Tidal channel geometry and optimisation constraints.

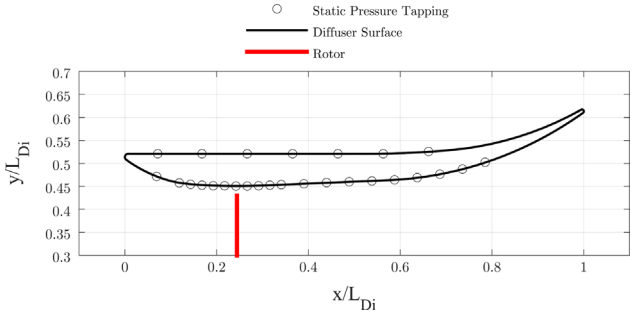

Fig. 4. Cross-section of the diffuser shape showing pressure tapping locations.

The complete rotor and diffuser geometries are detailed in a technical report available on the Durham University website (Cresswell et al., 2015).

2.5. Similitude

To ensure that the experimental setup was representative of tidal flow conditions it was necessary to ensure that conditions were matched. At its design operating conditions a device of the size detailed in Section 2.4 has a Reynolds number based on the throat diameter and freestream velocity of 2.53×10^7, which is unattainable in the test facilities used. Previous research suggests that testing at Reynolds numbers based on the throat diameter above 7.5×10^4 is sufficient to remove diffuser Reynolds effects (Cockrell and Markland, 1963; McDonald and Fox, 1966). The experiments presented here were conducted at Reynolds numbers greater than 5.25×10^5. The critical dimensions of the full and model scale devices are detailed in Table 2.

2.6. Experimental data set

The data presented here represent the highlights from an extensive experimental campaign investigating both steady and transient properties of diffuser augmented tidal stream devices performed by Cresswell (2015).

3. Yaw characteristics

3.1. Diffuser yaw

The effect of the yaw angle on the diffuser was examined by investigating the static pressure along its interior surface for a range of flow angles from $-45°$ to 45°. The static pressures within the diffuser can be seen in Fig. 6 for the half of the yaw traverse where the pressure tappings are located on the upwind side of the diffuser.

Fig. 6 shows that increased yawing of the flow causes changes in the diffuser's pressure distribution, leading to flow separation occurring closer to the leading edge of the diffuser, eventually

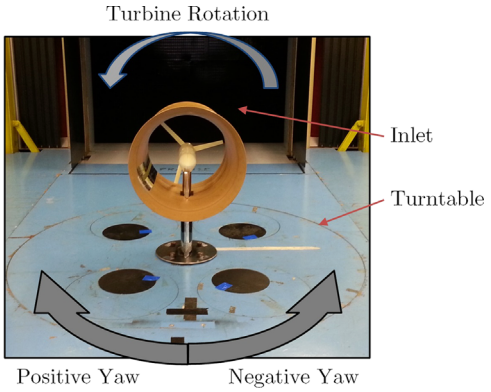

Fig. 5. Definition of yaw angle and turbine rotation for the diffuser and rotor.

Table 2
Critical dimensions of full scale and model scale devices.

Dimension	Full scale size (m)	Model scale size (m)
R_{Ro}	6.956	0.174
R_{Di}	10.000	0.250
L_{Di}	16.200	0.405

inducing diffuser stall. Increased yaw leads to a greater internal angle between the flow and the diffuser wall, causing greater diffusion within the forward section of the diffuser, leading to an adverse pressure gradient and a reduced flow velocity. With the reduced velocity there is insufficient boundary layer momentum for the flow to remain attached in the downstream diffuser section. This process can be seen in Fig. 6, where diffusion starts at $x/L_{Di} \approx 0.40$ at 0°, $x/L_{Di} \approx 0.16$ at 11° and $x/L_{Di} \approx -0.08$ at 23° with separation at $x/L_{Di} \approx 0.40$. Once flow yaw reaches 34°, the flow is completely detached from the diffuser and the diffuser has fully stalled. These diffuser stall angles are lower than those seen in Section 3.3 as diffuser optimisation was conducted with a rotor model and so relies on the tip gap jet to suppress trailing edge separation during generation.

3.2. Rotor yaw

The results for the variation of the rotor power coefficient with the tip speed ratio and yaw angle for a bare rotor are shown in Fig. 7 for the two blade pitches used in the tests. The greater the yaw angle, the more the power coefficient is reduced. The changing yaw angle of the rotor changes the local relative flow angle distribution around the rotor, the blade's angle of attack and therefore the power capture. The effect of the yaw angle on the power output of the bare rotor is more significant at greater yaw angles as would be expected given the greater deviations of the flow angles from the rotor design conditions. The effects of yaw on bare rotors are well documented and the reader is referred to Burton et al. (2011) for more information.

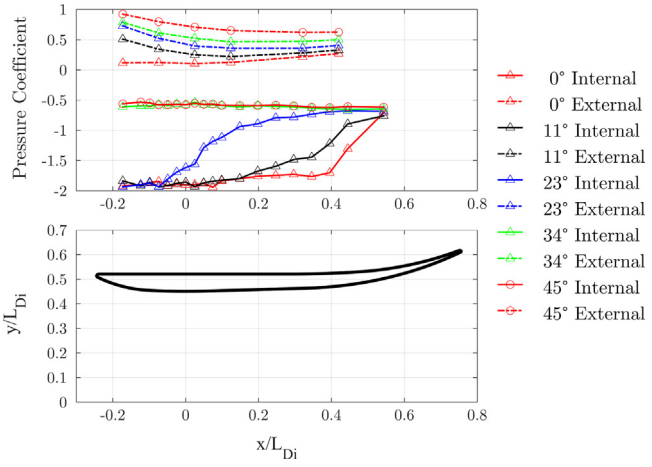

Fig. 6. Experimental static pressure coefficient around empty diffuser with variation of the yaw angle on upstream section, showing the diffuser geometry.

3.3. Combined yaw

The results for the variation of the power coefficient based on the rotor area with the tip speed ratio and yaw angle are shown in Fig. 8 for a Reynolds number, based on the freestream velocity and rotor diameter, of $Re = 5.1 \times 10^5$. The results show the diffuser's ability to sustain performance of the rotor at flows with yaw angles of up to ±30°.

The pressure coefficient around the diffuser for the yaw angles corresponding to Fig. 6 can be seen in Fig. 9. At 0° yaw the exterior pressure coefficients are negative at the leading edge due to the turbine thrust causing flow separation. As the yaw angle increases the exterior pressure also increases, which would be expected as the tappings are turning into the flow and the exterior separation is suppressed.

At yaw angles below 30°, the pressure coefficients within the rear of the diffuser ($x/L_{Di} > 0$) maintain a similar pressure distribution in all cases. Diffuser stall occurs at a yaw angle of just over 30°, with the onset of stall visible for the −5° blade pitch rotor at a diffuser yaw angle of 32°. This stall is evidenced by the separation of the flow diffuser at $x/L_{Di} \approx 0.46$ and the reduced peak power coefficient. At a yaw angle of 45°, the diffuser was fully stalled along the interior surface, leading to a significantly reduced power coefficient.

The diffuser's separation is prevented at low yaw angles by the tip gap jet, formed between the rotor and diffuser casing (Sanz et al., 2009), which acts to increase the boundary layer momentum and improve diffuser performance via a mechanism similar to circumferential blowing (Nicoll and Ramaprian, 1970; Kwong and Dowling, 1994). The performance maintenance of diffuser augmented turbines under yawed flows has been noted by Igra (1981) and Phillips (2003). Igra stated this to be due to increased lift generation by the annular wing section in yawed flows of ±15°. This assumes that the annular wing's lift increases to the point at which the diffuser and rotor combination stalls, which cannot explain the performance here as the diffuser stalls at angles of between 11° and 22°, as shown in Fig. 6, and so there must be another mechanism inducing the performance.

Phillips (2003) stated the performance was due to the slotted diffuser, with the slot flow adding momentum to the boundary

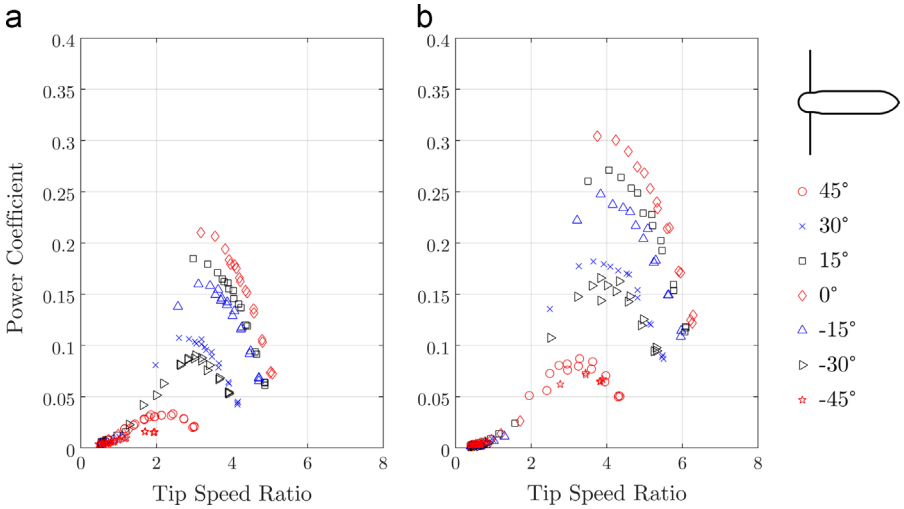

Fig. 7. Effect of yaw angle and tip speed ratio variation on the power coefficient for bare rotors at $Re = 5.1 \times 10^5$ (a) 0° blade pitch (b) −5° blade pitch.

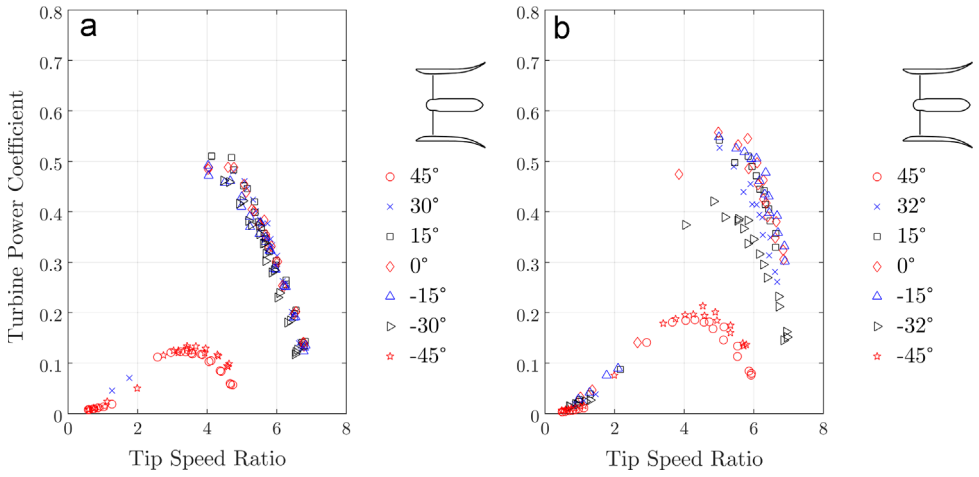

Fig. 8. Effect of the yaw angle and tip speed ratio on the power coefficient with (a) 0° blade pitch (b) −5° blade pitch rotors at a Reynolds number of $Re = 5.1 \times 10^5$.

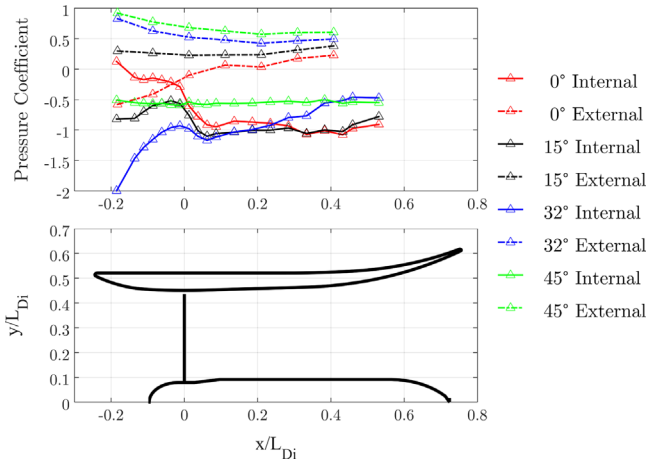

Fig. 9. Pressure coefficient around diffuser for diffuser and rotor case over yaw angle range, with −5° pitch blade, TSR=5, $Re = 5.5 \times 10^5$.

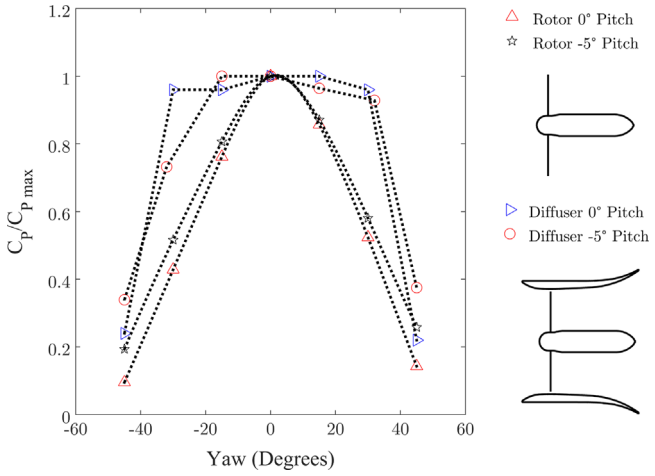

Fig. 10. Normalised peak power coefficient against the device yaw angle for both rotors with and without diffuser augmentation.

layer. This would explain the results seen by Phillips, but would again not explain the performance here as no slots are present. The separation suppression seen here must be due to the tip gap jet formed between the diffuser and the rotor adding momentum to the boundary layer. This separation suppression is the reason that the diffuser's "lift" and therefore rotor plane velocity are increased.

The stall phenomenon causes progressively decreasing power coefficients for yaw angles beyond ±30°, with a 2/3 reduction in the power coefficient by ±45° yaw. This ability to maintain performance at off angle flows is in contrast to a bare rotor as seen in Fig. 7. Here the decrease in the peak power coefficient relative to zero yaw is greater at all tested angles than when diffuser augmented. The normalised peak power coefficient's relationship to the yaw angle can be seen in Fig. 10 for both the bare and diffuser augmented cases.

Fig. 11 shows the maximum unaffected yaw angle of a variety of diffusers which have previously been tested at yaw. Also presented are results from Igra (1981), Phillips (2003) and Foreman and Gilbert (1979) of Grumman Aerospace.

The increasing performance range with the length to diameter ratio is due to the increased strength of the tip gap jet. The increased length enables a lower cavity pressure due to enhanced diffusion potential and a greater rotor plane velocity. With the reduced base pressure behind the rotor, stronger tip gap jets are generated and the diffuser is able to perform better in yawed flow due to enhanced wall attachment.

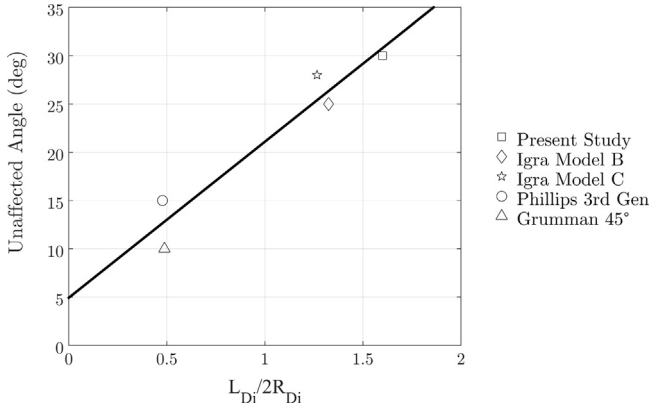

Fig. 11. Unaffected yaw angle against the diffuser length to diameter ratio.

The implications of the yaw behaviour of diffuser augmented turbines on the power generation characteristics and cost of energy are not straightforward and will depend upon the flow yaw present at the site and the cost of the device. Existing data from potential tidal stream sites (Blunden et al. 2008; Cornett, 2010; Sankaran Iyer, 2011), suggests that many tidal flows are rectilinear or close to rectilinear, meaning that the yaw properties will confer little benefit on diffuser augmented devices. For sites with higher flow yaw the potential is greater, though a comparison

of the costs and energy production of a diffuser augmented device and a bare rotor incorporating a yaw mechanism would be necessary to draw conclusions.

4. Wake structures

4.1. Rotor wake structure

Figs. 12 and 13 show the high losses and turbulence of the tip vortices and the associated velocity deficit and stagnation pressure losses seen in the tip region as well as the turbulence in the wake measured using a 5-hole pressure probe. The relatively low turbulence intensity of 2.11% in the test environment means that the wake takes some time to break down since the level of mixing between the wake and freestream flow is tied to the turbulence intensity (Hansen et al., 2011).

These distributions are expected as the blade geometry is such that the majority of work extraction occurs near to the blade tip, leading to the high velocity regions at the blade mid-span due to low power extraction and the low velocity at the tip caused by high extraction and tip losses.

4.2. Rotor wake recovery

The wake recovery rate is important for tidal stream turbines since it affects the wake's interactions with downstream turbines in an array and consequently dictates the minimum necessary turbine spacing. Wake recovery is quantified through the wake centreline axial velocity deficit (Stallard et al., 2011). The normalised velocity on the centreline of the -5° pitch rotor wake is shown in Fig. 14.

The velocity deficit in the bare rotor wake compares well with published data from flume tanks and water tunnels. The spread of data is due to the range of turbulence intensities, from 3% for Mycek et al. (2014) to 8% for Maganga et al. (2010), and variations in thrust and turbine model. Higher turbulence flows recovered more rapidly, as did flows with a lower thrust. The use of a uniform actuator disc, as with Myers and Bahaj (2010), tends to over predict the rate of wake recovery due to omission of swirl in the wake (Turnock et al., 2011).

The divergence of the results in the present study in the near wake is due to energy loses induced by the hub and blade roots removing energy from the flow and forming a combined wake which has a reduced velocity in proximity to the hub and in particular immediately downstream of the hub, as can be seen in Fig. 13. These results provide confidence in the ability of the experimental setup to accurately replicate hydrodynamic test setups.

4.3. Combined wake structure

The flow in the combined diffuser and rotor wake can be seen in Figs. 15 and 16. The flow is attracted to the interior diffuser walls by the tip gap jet flow and is caused to separate from the hub surface due to the adverse pressure gradient generated by the expansion. The tendency of the bulk flow to flow radially outwards from the axis leads to a region of low velocity flow behind the hub, around which the bulk flow passes.

The bulk flow through the rotor and the slow moving region of flow to the rear of the hub at diffuser exit interacts in phase with the rotor's rotation. The blade passing causes periodic radial expansion of the near hub velocity deficit region, forming a volume in which the mean velocity is low, with relatively large velocity fluctuations

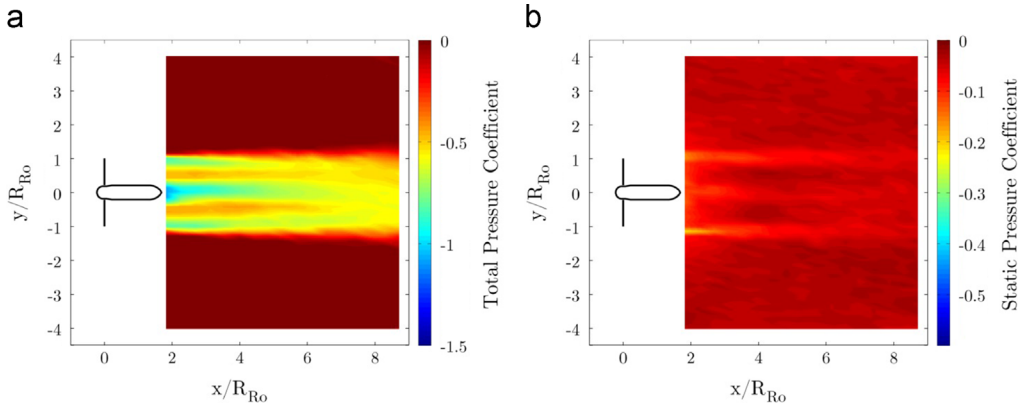

Fig. 12. (a) Total and (b) static pressure coefficients in the rotor wake for -5° blade pitch rotor at TSR=5.3 and $Re=4.9\times10^5$, on X–Y plane at turbine axis height.

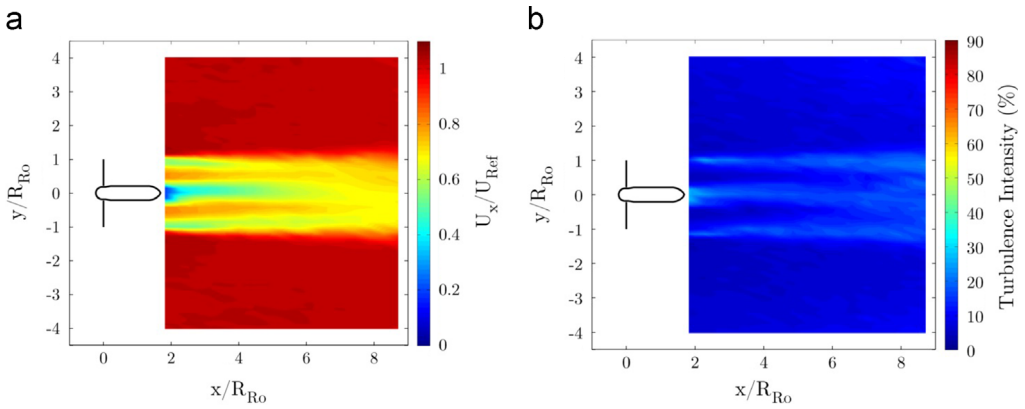

Fig. 13. (a) Normalised velocity and (b) turbulence intensity in the wake for -5° blade pitch rotor at TSR=5.3 and $Re=4.9\times10^5$, on X–Y plane at turbine axis height.

and a high resulting turbulence intensity. In the region near the diffuser casing the velocity remains high as the bulk flow is guided along the diffuser wall by the tip gap jet. In the region between the bulk flow and the hub wake flow a shear layer is formed which further adds to the turbulence seen in the flow. As seen in Fig. 15, the velocity deficit of the whole wake is significantly greater than for a bare turbine due to diffusion of the flow passing through the rotor. The pressure distributions seen in Fig. 16 show that the wake is significantly less energetic than in the bare rotor case as a result of diffuser pressure recovery and additional flow losses induced by the presence of the diffuser.

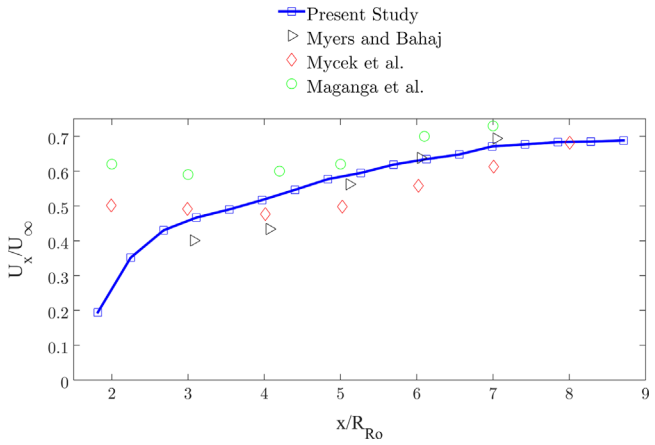

Fig. 14. Normalised velocity for -5° blade pitch rotor at $Re=5.5\times10^5$, with a turbulence intensity of 4.7% and tip speed ratio of 5.3, against published data (Maganga et al., 2010; Myers and Bahaj 2010; Mycek et al., 2014).

4.4. Combined wake recovery

The axial velocity deficit along the wake centreline of the -5° blade pitch, isolated rotor and the same rotor within the diffuser is shown in Fig. 17. The wake recovery is considerably slower in the case of the diffuser augmented turbine than the bare rotor. The velocity deficit in the diffuser augmented case was $\sim 0.65U_\infty$ at $x/R_{Ro}=9$, whereas with the bare rotor the velocity deficit was only $\sim 0.30U_\infty$ at $x/R_{Ro}=9$.

In the bare rotor the hub wake region is de-energised, but with a turbulence intensity of around 20% as seen in Fig. 13. The flow surrounding the hub wake is more energetic, although with a lower turbulence intensity. The proximity of the more energetic flow to the turbulent hub wake means that the two regions mix and the wake recovers rapidly.

In the diffuser augmented turbine, flow separates from the hub close to the turbine plane and there is a large region of slow moving, low energy flow behind the hub as seen in Figs. 15 and 16. Although this region has higher turbulence intensities than with the bare turbine, the surrounding flow also has low energy and so mixing, whilst strong, limits effective transmission of energy towards the wake centreline and therefore limits wake recovery.

The reduced wake recovery of diffuser augmented turbines means that the power generation characteristics of arrays of such devices will be adversely affected. These findings imply that streamwise array spacing would need to be increased to allow sufficient energy for economic extraction for downstream devices. Since the geographic extents of potential tidal stream sites are usually limited and that increased array spacing increases both connection and land lease costs this is detrimental to the case for the use of diffuser augmented turbines.

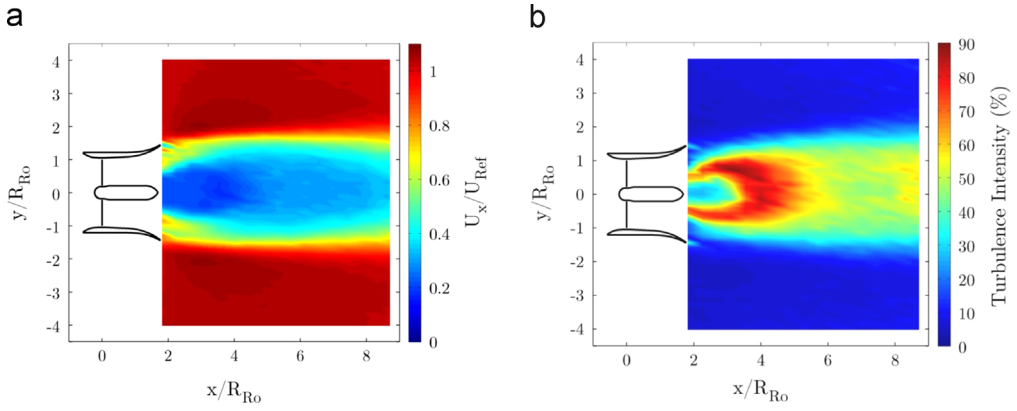

Fig. 15. (a) Normalised velocity and (b) turbulence intensity in the wake for -5° blade pitch rotor at TSR=5.3 and $Re=4.9\times10^5$, on X–Y plane at turbine axis height.

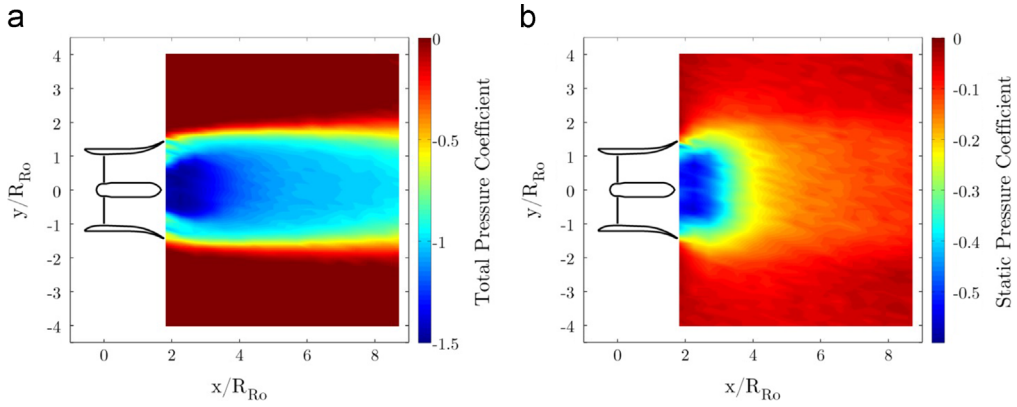

Fig. 16. (a) Total and (b) static pressure coefficients in the diffuser wake for -5° blade pitch rotor at TSR=5.5 and $Re=5.3\times10^5$, on X–Y plane at turbine axis height.

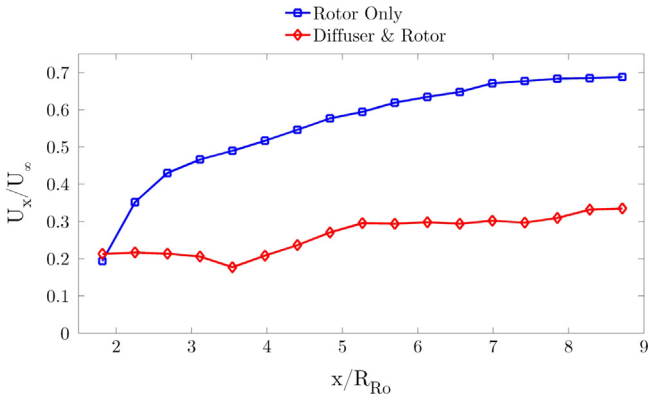

Fig. 17. Wake recovery for -5° blade pitch rotor and diffuser augmented rotor at $Re = 5.5 \times 10^5$, with a turbulence intensity of 4.7% and tip speed ratio of 5.3.

5. Conclusion

A generic diffuser geometry has been derived using an optimisation methodology based around Kriging surrogate modelling and a genetic algorithm. The output geometry has been combined with representative rotor geometry and the effects of flow yaw and device wake structures investigated. A data set for the study of diffuser augmented tidal stream turbines and numerical model validation has been generated.

The bare rotor was found to perform poorly under yawed flows, as suggested by the previous literature, but the diffuser augmented turbine was found to maintain performance at close to the peak level at yaw angles of up to $\pm 30^\circ$. This performance gain was found to be due to the sub-ambient cavity pressure in the diffuser sustained by the tip gap jet adding momentum to the boundary layer. The performance of diffuser augmented devices in yawed flows was found to be tied to the length to diameter ratio of the diffuser. The effects of the yaw performance on the ability of a diffuser augmented device to capture power in a yawed flow are potentially beneficial and are the subject of further work.

The wake recovery of diffuser augmented devices was found to be poor, with the wake velocity being less than half that of the bare rotor at 9 blade radii downstream. This reduced wake recovery implies that array spacing would need to be greater for diffuser augmented turbines. Diffuser augmented turbines are therefore less well suited to array deployment than are bare rotors, unless additional measures are taken to promote wake mixing.

Acknowledgements

Nick Cresswell was supported by Doctoral Funding from the EPSRC under award reference EP/P505488/1. The underlying data for this publication are openly available from the Durham University data archive at http://dx.doi.org/10.15128/gn91fk73x

References

Abe, K., Nishida, M., Sakurai, A., Ohya, Y., Kihara, H., Wada, E., Sato, K., 2005. Experimental and numerical investigations of flow fields behind a small wind turbine with a flanged diffuser. J. Wind Eng. Ind. Aerodyn. 93 (12), 951–970.

Bahaj, A.S., Myers, L.E. and Thompson, G. 2007. Characterising the wake of horizontal axis marine current turbines. In: Proceedings of the Seventh European Wave and Tidal Energy Conference.

Batten, W.M.J., Bahaj, A.S., Molland, A.F., Chaplin, J.R., 2007. Experimentally validated numerical method for the hydrodynamic design of horizontal axis tidal turbines. Ocean Eng. 34 (7), 1013–1020.

Bedard, R. 2005. Tidal in stream energy conversion (TISEC) devices–project definition study. Tidal in Stream Energy Conversion Feasibility Demonstration Project, Electric Power Research Institute. p. 185.

Belloni, C.S.K. and Willden, R.H.J. 2011. Flow field and performance analysis of bidirectional and open-centre ducted tidal turbines. In: Proceedings of the European Wave and Tidal Energy Conference, Southampton.

Blunden, L.S., Batten, W.M. and Bahaj, B.S. 2008. Comparing energy yields from fixed and yawing horizontal axis marine current turbines in the English channel. In: Proceedings of the ASME 2008 27th International Conference on Offshore Mechanics and Arctic Engineering, American Society of Mechanical Engineers.

Burton, T., Jenkins, N., Sharpe, D., Bossanyi, E., 2011. Wind Energy Handbook. John Wiley & Sons.

Callaghan, J.2006. Future marine energy: results of the marine energy challenge: cost competitiveness and growth of wave and tidal stream energy, Carbon Trust.

Cockrell, D.J., Markland, E., 1963. A review of incompressible diffuser flow: a reappraisal of an article by G. N. Patterson entitled 'Modern Diffuser Design' which was published in this journal twenty-five years ago. Aircr. Eng. Aerosp. Technol. 35 (10), 286–292.

Cornett, A. 2010. OES-IA guidance on assessing tidal current energy resources. In: Proceedings of the 3rd International Conference on Ocean Energy. Bilbao, Spain.

Crespo, A., Hernández, J., Frandsen, S., 1999. Survey of modelling methods for wind turbine wakes and wind farms. Wind Energy 2 (1), 1–24.

Cresswell, N.W., 2015. The Generation Potential of Diffuser Augmented Tidal Stream Turbines. University of Durham, Durham, UK, Doctoral thesis.

Cresswell, N.W., Ingram, G.L., Dominy, R.G., 2015. Durham Diffuser Augmented Tidal Stream Turbine Test Case. Durham University School of Engineering and Computing Sciences, Durham, UK.

Ewald, B. 1998. Wind Tunnel Wall Corrections (la Correction des effets de paroi en soufflerie), DTIC Document.

Flay, R., Nash, T., Phillips, D., 1998. Aerodynamic Analysis and Monitoring of the Vortec 7 Diffuser Augmented Wind Turbine. Institution of Professional Engineers New Zealand, Wellington, NZ.

Fleming, C.F., McIntosh, S.C. and Willden, R.H. 2011. Design and analysis of a bi-directional ducted tidal turbine. In: Proceedings of the 9th European Wave and Tidal Energy Conference, Southampton, UK.

Foreman, K.M., Gilbert, B.L., 1979. Further Investigations of Diffuser Augmented Wind Turbines Parts I and II. Grumman Research Department, New York.

Fraenkel, P.L., 2002. Power from marine currents. Proc. Inst. Mech. Eng. Part A 216 (1), 1–14.

Fraenkel, P.L.2007. Marine Current Turbines: An Update. All Energy 2007. Aberdeen.

Gaden, D.L.F., Bibeau, E.L., 2010. A numerical investigation into the effect of diffusers on the performance of hydro kinetic turbines using a validated momentum source turbine model. Renew. Energy 35, 1152–1158.

Garner, H.C., Rogers, E., Acum, W. and Maskell, E.1966. Subsonic wind tunnel wall corrections, DTIC Document.

Hansen, K.S., Barthelmie, R.J., Jensen, L.E., Sommer, A., 2011. The impact of turbulence intensity and atmospheric stability on power deficits due to wind turbine wakes at Horns Rev wind farm. Wind Energy 15 (1), 183–196.

Harrison, M.E., Batten W.M.J., Myers, L.E. and Bahaj, A.S. 2009. A comparison between CFD simulations and experiments for predicting the far wake of horizontal axis tidal turbines. In: Proceedings of the 8th European Wave and Tidal Energy Conference.

Igra, O., 1977. Compact shrouds for wind turbines. Energy Convers. 16 (4), 149–157.

Igra, O., 1981. Research and development for shrouded wind turbines. Energy Convers. Manag. 21 (1), 35.

Jeong, S., Murayama, M., Yamamoto, K., 2005. Efficient optimization design method using Kriging model. J. Aircr. 42 (2), 413–420.

Khan, M.J., Bhuyan, G., Iqbal, M.T., Quaicoe, J.E., 2009. Hydrokinetic energy conversion systems and assessment of horizontal and vertical axis turbines for river and tidal applications: a technology status review. Appl. Energy 86 (10), 1823–1835.

Kogan, A., Seginer, A., 1963. Shrouded Aerogenerator Design Study II: Axisymmetrical Shroud Performance, Department of Aeronautical Engineering. Technion - Israel Institute of Technology, Haifa, Israel.

Kwong, A.H.M., Dowling, A.P., 1994. Active boundary-layer control in diffusers. AIAA J. 32 (12), 2409–2414.

Lawn, C.J., 2003. Optimization of the power output from ducted turbines. Proc. Inst. Mech. Eng. Part A 217 (1), 107–117.

Li, M., 2008. An improved Kriging assisted multi-objective genetic algorithm. J. Mech. Des. 130, 825–836.

Lophaven, S.N., Nielsen, H.B., Sondergaard, J., 2002. DACE: A Matlab Kriging Toolbox. Technical University of Denmark, Lyngby, Denmark.

Luquet, R., Bellevre, D., Fréchou, D., Perdon P., Guinard, P. and Goujon, G. 2011. Design and model testing of an optimised ducted marine current turbine. In: Proceedings of the European Wave and Tidal Energy Conference, Southampton.

Maganga, F., Germain, G., King, J., Pinon, G., Rivoalen, E., 2010. "Experimental characterisation of flow effects on marine current turbine behaviour and on its wake properties."Renew Power Gener. IET 4 (6), 498–509.

McDonald, A.T., Fox, R.W., 1966. An experimental investigation of incompressible flow in conical diffusers. Int. J. Mech. Sci. 8 (2), 125–139.

Munch, C., Vonlanthen, M., Gomes, J., Luquet, R., Guinard, P. and Avellan, F. 2009. Design and performance assessment of a tidal ducted turbine. In: Proceedings of the 3rd IAHR International Meeting of the Workgroup on Cavitation and Dynamic Problems in Hydraulic Machinery and Systems. Brno, Czech Republic.

Mycek, P., Gaurier, B., Germain, G., Pinon, G., Rivoalen, E., 2014. Experimental study of the turbulence intensity effects on marine current turbines behaviour. Part I: one single turbine. Renew. Energy 66 (0), 729–746.

Myers, L.E., Bahaj, A.S., 2010. Experimental analysis of the flow field around horizontal axis tidal turbines by use of scale mesh disk rotor simulators. Ocean Eng. 37 (2–3), 218–227.
Nicoll, W.B., Ramaprian, B.R., 1970. Performance of conical diffusers with annular injection at inlet. J. Fluids Eng. 92 (4), 827–835.
Oettle, N., 2013. The Effects of Unsteady On-Road Flow Conditions on Cabin Noise. Durham University, Durham, UK, Doctoral thesis.
Ohya, Y., Karasudani, T., 2010. A shrouded wind turbine generating high output power with wind-lens technology. Energies 3 (4), 634–649.
Ohya, Y., Karasudani, T., Sakurai, A., Abe, K.-i., Inoue, M., 2008. Development of a shrouded wind turbine with a flanged diffuser. J. Wind Eng. Ind. Aerodyn. 96 (5), 524–539.
Ohya, Y., Uchida, T., Karasudani, T., Hasegawa, M., Kume, H., 2012. Numerical studies of flow around a wind turbine equipped with a flanged-diffuser shroud using an actuator-disk model. Wind Eng. 36 (4), 455–472.
Oman, R.A., Foreman, K.M. and Gilbert, B.L. 1977. Investigation of Diffuser-Augmented Wind Turbines, Parts I & II. New York: 118.
Phillips, D.G., 2003. An Investigation on Diffuser Augmented Wind Turbine Design. University of Auckland, Auckland, New Zealand, Doctoral thesis.
Reinecke, J., von Backström, T.W. and Venter, G. 2011. Effect of a diffuser on the performance of an ocean current turbine. In: Proceedings of the European Wave and Tidal Energy Conference. Southampton.
Sankaran Iyer, A., 2011. New Methodologies and Scenarios for Evaluating Tidal Current Energy Potential. Edinburgh University, Edinburgh, UK, Doctoral thesis.
Sanz, W., M. Kelterer, R. Pecnik, A. Marn and E. Gottlich 2009. Numerical investigation of the effect of tip leakage flow on an aggressive s-shaped intermediate turbine duct. ASME Turbo Expo 2009: Power for Land, Sea, and Air, American Society of Mechanical Engineers.
Sharqawy, M.H., Lienhard, J.H., Zubair, S.M., 2010. Thermophysical properties of seawater: a review of existing correlations and data. Desalin. Water Treat 16 (1–3), 354–380.
Shives, M., Crawford, C., 2010. Overall efficiency of ducted tidal current turbines. Oceans, 2010.
Sorensen, J.N., 2011. Aerodynamic aspects of wind energy conversion. Annu. Rev. Fluid Mech. 43 (1), 427–448.
Stallard, T., R. Collings, T. Feng and J. Whelan2011. Interactions between tidal turbine wakes: experimental study of a group of 3-bladed rotors. In: Proceedings of the 9th European Wave and Tidal Energy Conference, Southampton, U.K.
Turnock, S.R., Phillips, A.B., Banks, J., Nicholls-Lee, R., 2011. Modelling tidal current turbine wakes using a coupled RANS-BEMT approach as a tool for analysing power capture of arrays of turbines. Ocean Eng. 38, 1300–1307.
van Bussel, G.J.W., 2007. The science of making more torque from wind: diffuser experiments and theory revisited. J. Phys.: Conf. Ser. 75 (1), 012010.
Vermeer, L.J., Sørensen, J.N., Crespo, A., 2003. Wind turbine wake aerodynamics. Prog. Aerosp. Sci. 39 (6–7), 467–510.